Identifying Plausible Harmful N-k Contingencies: A Practical Approach based on Dynamic Simulations

Tilman Weckesser
Center for Electric Power and Energy (CEE)
Technical University of Denmark (DTU)
Lyngby, Denmark
jtgw@elektro.dtu.dk

Thierry Van Cutsem
Fund for Scientific Research (FNRS)
at the University of Liège
Liège, Belgium
t.vancutsem@uliege.be

***Abstract*—This paper presents a practical search algorithm using detailed dynamic simulations to identify plausible harmful $N-k$ contingency sequences. Starting from an initial list of contingencies, progressively more severe contingency sequences are investigated. For that purpose, components, which violated conservative protection limits during a $N-k$ contingency simulation are identified and considered as candidate $k+1$-th contingencies, since these could be tripped due to a hidden failure. This approach takes into account cascading events, such as over- or under-speed generator tripping, which are considered to be part of the system response. The implementation of the proposed algorithm into a parallel computing environment and its performance are demonstrated on the IEEE Nordic test system.**

***Index Terms*—N-k contingencies, cascading events, protection hidden failures, time-domain simulation.**

I. Introduction

The integration of distributed generation from fluctuating energy sources and delays in the reinforcement of the grid, due to e.g. public objection, result in more frequent operation of the power system closer to its limits. This may trigger cascading events, due to e.g. component overloading. In order to ensure uninterrupted power delivery, system protection designers need to develop effective, automatic emergency control schemes (also referred to as System Integrity Protection Schemes - SIPS) against those events, which are rare but have a large impact. For that purpose, identification of plausible and harmful $N-k$ contingency sequences is crucial.

Due to the large number of possible contingencies and their combinations, identification of harmful $N-k$ contingency sequences with brute force approaches is infeasible.

In [1], the IEEE Cascading Failure Working Group concludes that the mechanims and the details, which need to be modeled in cascading failure studies, are not yet understood and, hence, further research is needed.

One approach for identifying plausible cascading events is based on the simulation of an initial fault and the subsequent construction of a cascading event tree involving plausible outages. These cascading outages can for example be caused by hidden failures, which have played a key role in many catastrophic power system failures [2] and can be due to outdated protection settings, equipment failure or undue tripping of overloaded equipment. The approach of constructing a cascading event tree is for example used in [2], [3] and [4]. Probabilities are assigned to the individual events and a branch of the tree is explored until the probability of the event sequence falls below a pre-defined threshold or unacceptable system conditions are identified.

In [5], a new vulnerability index was proposed and used to determine the degree of vulnerability of transmission lines and sections in a power system. For that purpose, Fault Chain theory from the field of Security Sciences is applied.

An approach for identifying minimal $N-k$ contingencies triggering large cascading failures based on a "Random Chemistry" algorithm was proposed in [6]. Based on the observation that a relatively small number of components contribute disproportionately to system vulnerability, the general idea is to randomly pick a large set of contingencies S_0 causing cascading failures and find the smallest subset, which still causes system failure. If a randomly selected subset triggers cascading failures, then it replaces the larger set S_0. This procedure is repeated until a subset with the desired size k_{max} is found. To further reduce its size and identify a minimum number of contingencies to cause system failure, a pruning approach is used, which removes individual contingencies from the subset and simulates it.

A data driven approach was proposed in [7]. The method utilizes data from many cascading failure simulations to determine an influence graph. This graph provides information on how cascades evolve in a particular system and allows to identify modifications that will reduce cascade propagation.

In [8] the method for identifying high risk $N-k$ contingencies is based on a graph. Functional groups are defined, which are made up of components that are operating and failing together, due to the connection structure and protection scheme. Moreover, interfacing components are defined as breakers and open switches. In the resulting graph, the nodes are functional groups and the edges are interfacing components. Then, rare event approximation and event trees are used to determine high-risk $N-k$ contingencies.

The approach proposed in [9] relies on pattern recognition and fuzzy estimation for on-line identification of an event sequence, which may lead to catastrophic failure. For that purpose, probable contingency sequences are investigated off-line using power flow computations and then the results are utilized on-line to identify a critical collapse sequence.

Lastly, the authors of [10] evaluated a number of existing methods for real-time applications.

In this paper, an extended, generalized and improved version of the $N-k$ search algorithm presented in [11], is proposed. While in [11] plausible harmful $N-k$ contingency sequences were identified based on comparison of steady-state values, in this paper identification of plausible contingencies is based on detailed dynamic time simulations.

The remaining of the paper is structured as follows. In Section II, the search algorithm, its implementation into a parallel processing environment as well as its modification under consideration of limited computational resources are presented. Results obtained from simulations of the IEEE Nordic Test System are shown in Section III. Finally, some concluding remarks are offered in Section IV.

II. Search approach for identifying plausible harmful N-k contingencies

A. Detailed procedure

In Fig. 1, a flow chart of the proposed algorithm is presented. The grey dashed blocks are only considered when limited computational resources are available, which will be discussed in Section II-E. As an input the proposed approach receives a time-domain model of the power system and an initial list of contingency sequences. A contingency sequence C_i consists of one or more individual contingencies, such as generator or transmission line outages. The power system model includes models of protective relays, which monitor certain quantities and disconnect components to avoid e.g. under- or over-speed of synchronous machines, overloading of transmission lines, etc. Consequently, the system response to an applied contingency sequence may include Cascading Events (CEs), such as transmission line tripping triggered by power system protections, as defined in [12]. It should be noted that cascading events in terms of tripping of components, correspond to intentional interventions of the protection systems.

The procedure is as follows. L is a list of $N-k$ contingency sequences, which contains all sequences to be investigated. The length of the list is changing, since new plausible contingency sequences are added, and assessed sequences are removed. The list L is initialized with the aforementioned contingency sequences. While the list is not empty the next entry C_i is extracted. Then, a time-domain simulation is performed starting from the initial system operating point and the individual contingency $c_m \in C_i$ are applied consecutively, separated with a short-delay Δt, or at pre-defined times. During the simulation, system states are monitored and the simulation is terminated, if an instability is identified or a new steady-state operating point is reached. If the contingency sequence C_i led to an instability, it is stored in the list of unstable contingencies L_u and, if the new steady-state is non-viable, then it is added to the list L_w of contingency sequences leading to weak operating conditions. On the other hand, if the system remained stable after C_i was applied, the final steady state is viable and k_i (the number of individual contingencies in C_i) is smaller than a pre-defined maximum number k_{max},

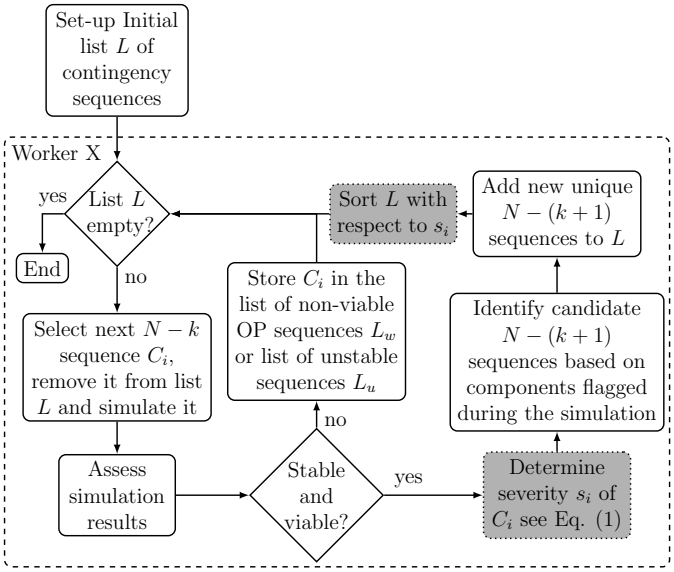

Figure 1. Flow chart of the search algorithm. Functions in grey dotted boxes are introduced in Section II-E

then it is checked whether candidate k_i+1-th contingencies were identified during the simulation (see Section II-B).

Based on the contingencies, candidate $N-(k_i+1)$ contingency sequences are derived. If both questions hereafter are answered in the negative, the candidate sequences are added to the list L:

- Does the candidate $N-(k_i+1)$ sequence contain exactly the same individual contingencies as an already assessed $N-k_n$ sequence?
- Was a subset of individual contingencies of the candidate $N-(k_i+1)$ sequence already found to result in instability or non-viable operating condition?

In the above procedure, the contingency sequences are treated as unordered sets, i.e. the order of the individual contingencies in a sequence is neglected in the comparisons.

The described procedure is continued until all contingency sequences in L were investigated and the list is empty.

B. Identification of candidate $(k+1)$-th contingency

Certain components are monitored during the time-domain simulation. Candidate $(k+1)$-th contingencies may be triggered by a Hidden Failure (HF), as defined in [13], in the protection system. The HF causes the protected component to be tripped although the monitored variable did not exceed the associated protection limit. It should be emphasized that in contrast to CEs, where a component is assumed to be tripped due to violation of a limit, HFs cause unintentional trippings, due to malfunctioning of protective relays.

Two examples are shown in Fig. 2. Figure 2a shows the post-disturbance evolution of the field current i_{fd} of a generator equipped with an OverExcitation Limiter (OEL). In normal operation, when i_{fd} exceeds the limit i_{fd}^{lim}, the OEL would limit it after a delay. However, an HF could cause the generator to be tripped after a delay T_l^{OEL}, when i_{fd} exceeds

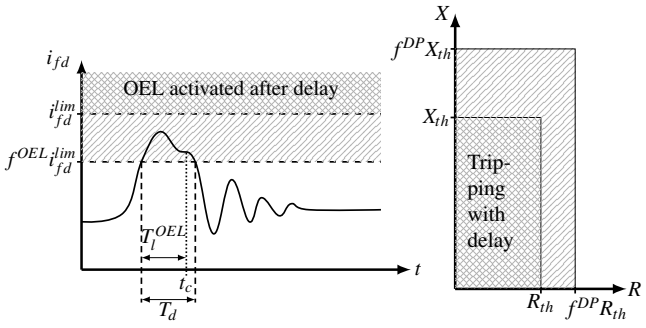

(a) Generator (b) Transmission line

Figure 2. Visualization of identification of candidate $k+1$-th contingencies.

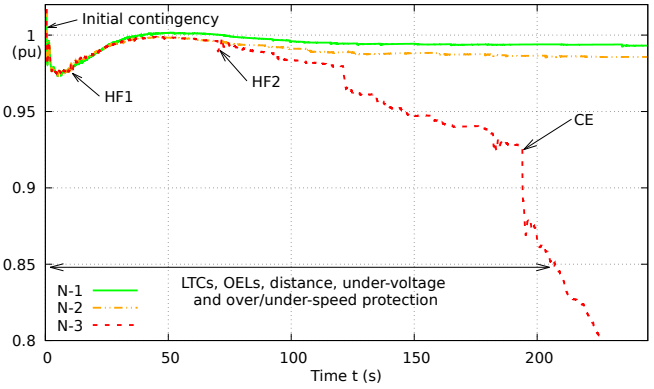

Figure 3. Illustration of $N-k$ search approach - Voltage evolution after applying $N-1$, $N-2$ and $N-3$ contingencies. (LTC: Load Tap Changer)

a value, which is by a factor of f^{OEL} smaller than i_{fd}^{lim}. In the proposed approach, a protected generator is flagged as candidate $(k+1)$-th contingency, when i_{fd} remains above the limit $f^{OEL} i_{fd}^{lim}$ for longer than T_l^{OEL}. In a subsequent $N-(k+1)$ contingency sequence, an outage of the generator will be considered as a HF applied at the time t_c defined in Fig. 2a.

Similarly, a Distance Protection (DP) could trip the respective transmission line after a delay T_l^{DP}, when the measured apparent impedance enters a protection zone, which is by a factor of f^{DP} larger than the actual zone (see Fig. 2b).

C. Illustrative example

In Fig. 3 an illustrative example of the proposed approach is shown. First, an initial $N-1$ contingency is simulated (green solid curve). During the simulation, a component is flagged and considered as HF1 in the $N-2$ case (dashed and dotted orange curve). A second component is flagged and considered as HF2 in the $N-3$ contingency (dashed red curve). This results in a voltage collapse after triggering of a CE.

Note that all three curves coincide until the time of HF1, while the orange and the red curves coincide until the time of HF2.

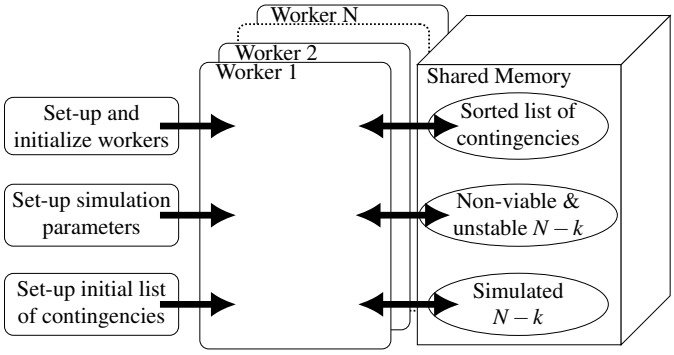

Figure 4. Implementation into parallel computing environment

D. Implementation into a parallel computing environment

Since every C_i in L can be simulated and assessed individually, a parallel processing approach is proposed to speed up the assessment. This is sketched in Fig. 4. A pool of workers is set-up and initialized, whose number depends on the available hardware. Some of the data such as the lists L, L_u, L_w and a list of already simulated contingencies need to be accessed by all workers. Hence, these are stored in shared memory which all workers, one at a time, can access. After initialization, each worker runs the part of the algorithm discussed in Section II-A, which is inside the dashed box in Fig. 1.

E. Consideration of limited available computational resources

So far it was assumed that sufficient computational resources were available to investigate all plausible contingency sequences. However, if those resources are limited, then it is preferable to first investigate the most harmful contingency sequences. For that purpose, it is proposed to determine the severity of each simulated stable $N-k_i$ case in terms of a suitable severity index. Under the assumption, that a subsequent $N-(k_i+1)$ contingency sequence will further deteriorate the system conditions, it is suggested to assign the severity of the $N-k_i$ case to all the identified $N-(k_i+1)$ sequences. In order to first investigate the most severe cases, the contingency sequences in the list L are sorted according to the proposed index.

The severity index should be such that a higher value is attributed to a situation which, under the effect of the next disturbance, is more likely to degenerate into instability or be subject to additional CEs. Various indices can be thought of. In the simulations reported in this paper, it was chosen to observe the final degradation of bus voltages, evaluated by the following index:

$$s_i = \frac{1}{k_i} \sum_{b \in B} [\max(0, V_b(t_0) - V_b(t_e))]^2 \qquad (1)$$

where B is the set of all buses in the system or in the area of interest, t_0 the time before the first disturbance is applied and t_e the time at the end of the simulation. It is expected that a larger value of s_i corresponds to a more severe situation. The max-function ensures that only buses are

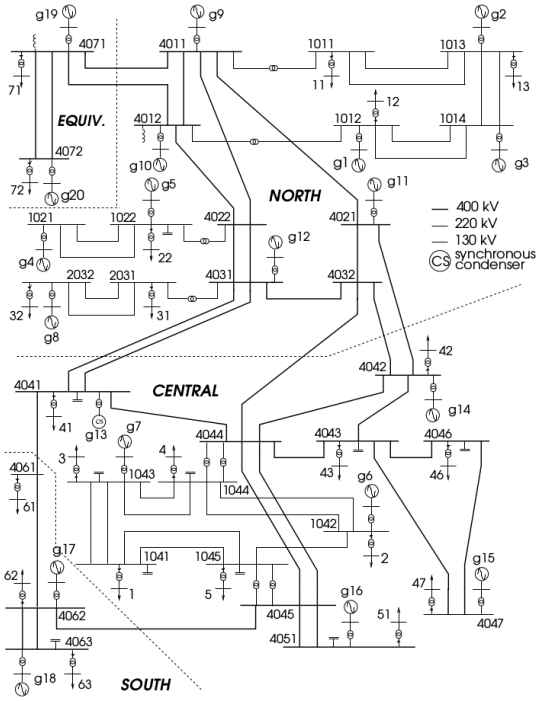

Figure 5. One-line diagram of the IEEE Nordic test system [14]

considered, where the voltage magnitude has been depressed. Moreover, the square of the deviation is used to increase the weight of large deviations. Finally, in order to favour a sequence with small number of contingencies and a breadth-first search like inspection of the event tree, the sum of squared voltage deviations is divided by the number of contingencies k_i applied to the system between times t_0 and t_e.

This results in the introduction of the grey dotted boxes in Fig. 1. In this version, if the simulation is stable and the final operating point is viable, then the severity s_i is computed and, after adding the new unique $N-(k+1)$ contingency sequence, the list L is sorted with respect to s_i.

It should be noted that, while this severity index is appropriate for voltage instability, for angular or frequency instability investigations, it may be necessary to consider a different index.

III. Simulation results

A. IEEE Nordic Test System

In this section, the Nordic test system, set up by the IEEE Task Force on "Test Systems for Voltage Stability and Security Assessment", is used to demonstrate the performance of the proposed $N-k$ search algorithm. The detailed data as well as the operating points can be found in [14]. A one-line diagram is shown in Fig. 5. All MV loads are served through distribution transformers equipped with LTCs. Contrary to [14] the LTCs do not have constant tapping delays, but variable delays with an inverse-time characteristic.

To simulate CEs and HFs, the following component protections were added.

1) Generator protection: All generators are protected with a simple over-/under-speed protection relay and an under-voltage protection relay.

a) Over-/under-speed protection: The protection trips the respective generator instantaneously, if its rotor speed exceeds ± 8 % of nominal value.

b) Under-voltage (UV) protection: The protection considers two thresholds. If the terminal voltage drops below 0.9 pu, but stays above 0.8 pu, the generator is tripped with a delay of 30 s. If the voltage falls below 0.8 pu, it is disconnected instantaneously.

2) Transmission line protection: Each line is protected by a distance protection relay. The settings of the relay are derived based on the MVA capacity of the line and give a resistance R_{th} and a reactance X_{th} threshold. If the resistance R and reactance X calculated at any end of the protected line remain inside the rectangle defined by $(0,0)$, $(0,X_{th})$, (R_{th},X_{th}) and $(R_{th},0)$ longer than T_l^{DP} then the line is tripped (see Fig. 2b).

3) Identification of candidate $(k+1)$-th contingencies: In order to identify transmission lines, which are plausible candidates for $(k+1)$-th contingencies, the time T_l^{DP} was chosen equal to 2.3 s and f^{DP} was chosen equal to 3.5. The corresponding factor f^{OEL} for identifying candidate generators was chosen equal to 0.95 and the time T_l^{OEL} was set to 0.5 s (see Fig. 2a). These factors and times were selected to have a sufficient number of HFs and, hence, demonstrate the method. Moreover, the chosen values were inspired by discussions with two transmission system operators.

B. Operating points

The proposed method is tested on different operating points, which are described in detail in [14].

- **Operating point B:** Operating Point (OP) B is a $N-1$ secure operating point.
- **Operating points B plus $50-400$ MW:** Additional six OPs are considered, where the loading of the Central region (see Fig. 5) has been uniformly increased by a total of 50, 100, 250, 300, 350 and 400 MW, respectively. This leads to an increased power flow from the North to the Central region and further stresses the system.

The initial list of contingencies contains all generators (except $g20$, which is an equivalent accounting for the connection to an external system) and all transmission lines. The contingencies are applied as follows:

- generator: tripping at time $t = 1.0$ s
- transmission line: three-phase short-circuit close to one end of the line at $t = 1.0$ s, cleared after 150 ms (t=1.15 s) through tripping of the faulted line.

Up to three contingencies ($k_{max} = 3$) are considered. It should be recalled that a $N-3$ case consists of one contingency from the initial list of contingencies plus two hidden failures (HF1 and HF2), where HF1 was identified in the preceding $N-1$ case and HF2 in the preceding $N-2$ case. Cascading events are considered to be part of the system response and are not counted, when determining k.

TABLE I
OVERVIEW OF RESULTS WITH INCREASING LOADING LEVEL.

Operating point	Nb. of simul.	Unstable				Non-viable
		$N-1$	$N-2$	$N-3$	*all*	
B	411	0	31	67	98	4
B plus 50 MW	395	3	32	53	88	2
B plus 100 MW	438	4	41	71	116	2
B plus 250 MW	368	9	47	43	99	6
B plus 300 MW	421	11	37	50	98	6
B plus 350 MW	479	11	53	67	131	6
B plus 400 MW	488	14	57	70	141	9

A case is considered unstable, when the voltage at one bus drops below 0.6 pu and remains below this threshold for at least 500 ms. When an instability is detected the simulation is terminated. The criterion for identification of a non-viable operating point is as follows: in the final steady state the voltage magnitudes of at least *five* buses lie below 0.85 pu.

C. Performance with sufficient computational resources

Table I gives an overview of the number of simulations, identified unstable and non-viable cases for the various loading levels. It can be observed that the number of unstable cases and non-viable cases generally increases with the loading level. While the original OP B is $N-1$ secure, the number of unstable $N-1$ contingencies increases steadily up to 14 in OP B plus 400 MW. A decrease of the total number of identified unstable cases after a loading increase, e.g. from OP B to OP B plus 50 MW may be explained by the simultaneous increase of $N-1$ and $N-2$ unstable cases. Each additional unstable $N-1$ contingency results in the elimination of all unstable $N-2$ and $N-3$ contingency sequences, which contain this now unstable $N-1$ contingency. Similarly, each new unstable $N-2$ contingency sequence eliminates all unstable $N-3$ sequences of which this $N-2$ contingency sequence is a subset.

1) Example - unstable case - long-term voltage instability: The procedure when identifying an unstable $N-3$ contingency sequence is illustrated hereafter. Figure 6 shows the voltage evolution at bus 1044, where an $N-3$ contingency results in unacceptably low voltages. The graph also shows the voltage evolution in the preceding $N-1$ and $N-2$ case simulations. The green solid curve is the voltage response, when only the initial disturbance occurs, which is the loss of generator $g14$. It can be observed that the contingency leads to a depressed bus voltage with a final value of 0.933 pu. During the N-1 contingency simulation, the field currents of all generators and the apparent impedance from all transmission lines are monitored to identify a plausible second contingency. In this case, the tripping of line $1011-1013$ was determined as one plausible HF.

Figure 7 shows the evolution of the corresponding apparent impedance. The evolutions from the $N-1$ and $N-2$ simulations are presented. With $f^{DP}R_{th} = 64.9\ \Omega$, the

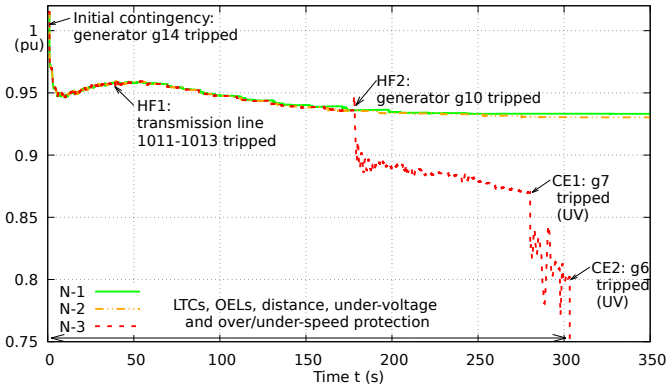

Figure 6. Bus 1044 - Voltage evolution for $N-1$, $N-2$ and $N-3$ contingency sequence identified with the proposed algorithm.

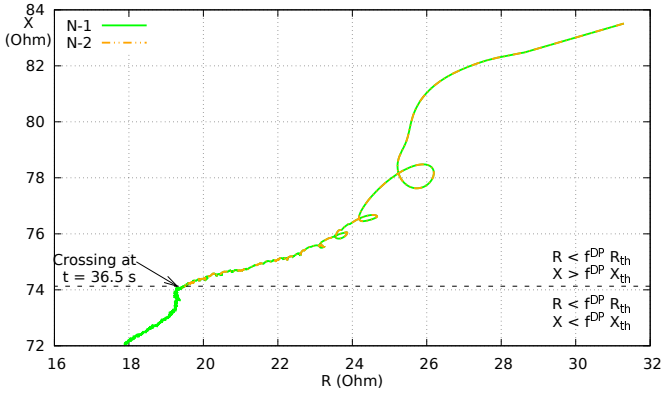

Figure 7. Transmission line $1011-1013$ - Apparent impedance evolution for $N-1$ and $N-2$ contingency sequences identified with the proposed algorithm.

resistance is from the beginning below this limit, while the value of the reactance is still larger than $f^{DP}X_{th}$. After the initial disturbance, the apparent impedance moves towards the limit $f^{DP}X_{th}$ and eventually crosses it at $t = 36.5$ s. Since it remains below the threshold for longer than 2.3 s, it is flagged as a candidate HF taking place at 38.8 s. Consequently, in a subsequent $N-2$ simulation, transmission line $1011-1013$ is tripped as HF1 at $t = 38.8$ s. This case is shown by the orange dashed-dotted curve in Figs. 6 and 7. The tripping of the line results in a slightly more depressed voltage magnitude at bus 1044 with a final value of 0.930 pu.

Also during the $N-2$ contingency simulation, the field currents of the generators and the apparent impedance in the lines are monitored to identify a plausible second HF.

In Fig. 8, the evolution of the field current of generator $g10$ is shown extracted from the simulations of the $N-1$, $N-2$ and $N-3$ contingency sequences. In the graph, the limit $f^{OEL}i_{fd}^{lim}$ is indicated by the black dashed line. It can be observed that, in the $N-1$ contingency simulation (green solid curve), the field current increases after the initial disturbance, but settles at 1.8 pu, which is below the limit $f^{OEL}i_{fd}^{lim}$. The dashed-dotted orange curve shows the field current evolution extracted from the simulation of the $N-2$ contingency sequence. The tripping

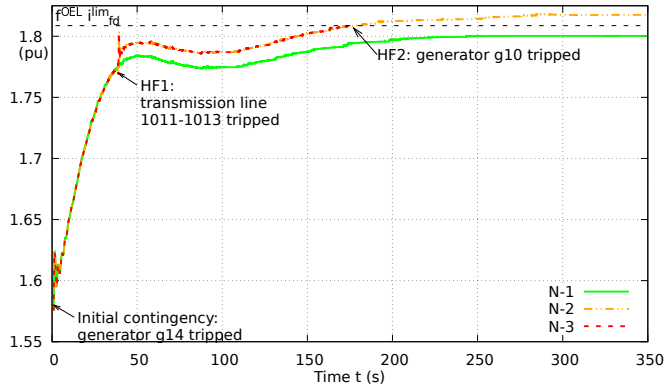

Figure 8. Generator $g10$ - Field current evolution for $N-1$, $N-2$ and $N-3$ contingency sequences identified with the proposed algorithm.

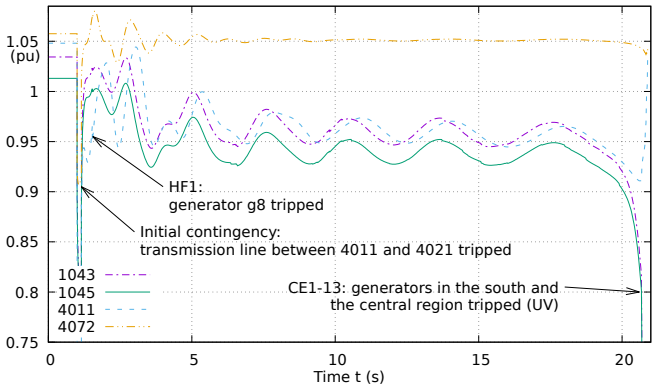

Figure 9. Evolution of selected bus voltages in central and northern region.

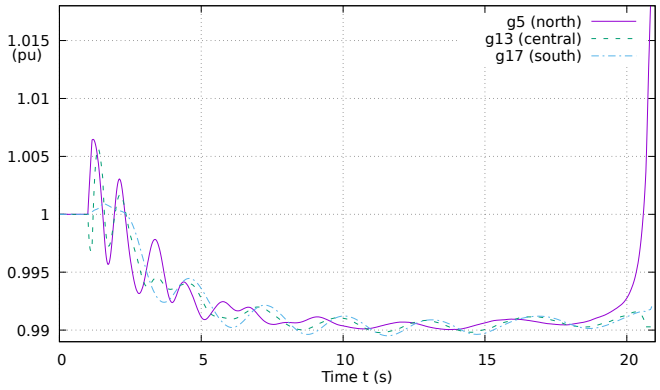

Figure 10. Evolution of selected generator speeds in southern, central and northern region.

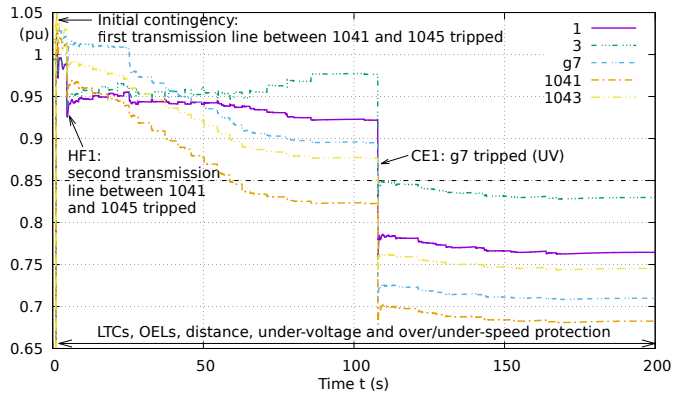

Figure 11. Voltage evolution at buses with lowest final steady state voltage in non-viable case.

of line $1011-1013$ (HF1) and the resulting degradation of the operating condition require a further increase of the field current of $g10$. Figure 8 shows that it exceeds the limit at t=177.1 s. Since it remains above this limit, the generator $g10$ is marked as candidate third contingency after T_l^{OEL} (0.5 s). In a subsequent $N-3$ contingency sequence simulation, generator $g10$ is tripped as HF2, which corresponds to the red dashed curve in Figs. 6 and 8.

In Fig. 6, it can be observed that this second HF leads to a severe voltage drop at bus 1044. Subsequently, the system undergoes two cascading events, namely under-voltage tripping of generator $g7$ at 280.3 s and $g6$ at 303.3 s. Immediately after the second CE a voltage collapse takes place.

2) Example - unstable case - rotor-angle instability: Figure 9 shows the voltage evolution at selected buses in another identified unstable $N-2$ case. The initial contingency is the loss of the transmission line between buses 4011 and 4021. During the simulation of the corresponding $N-1$ case, amongst other candidate contingencies, the loss of generator g8 is identified as a plausible $(k+1)$-th contingency. This generator is not in the direct neighborhood of the first contingency and the combination of those two contingencies would probably not be considered from simple inspection of the network graph. In Fig. 9, it can be observed that the initial contingency plus HF1 cause severe degradation of the system condition. Eventually this triggers 13 CEs, the under-voltage tripping of all generators in the central and southern region.

The underlying instability mechanism is rotor-angle instability. Figure 10 shows the rotor speed evolution of selected generators in the northern, central and southern region. The generator separation is easily seen. The latter is responsible for the 13 CEs mentioned above (i.e. the system already shows instability before the generators are tripped).

3) Example - non-viable case: In the non-viable case illustrated hereafter, a contingency sequence leads to unacceptably low final voltages at a number of buses, but no voltage collapse. The voltage evolutions at selected buses are shown in Fig. 11. The $N-2$ contingency sequence consists of the fault induced tripping of the first line $1041-1045$ as initial contingency followed by the outage of the second line $1041-1045$ at 4.7 s as a HF. This series of contingencies causes severe degradation of the system conditions and triggers a cascading event (CE1) corresponding to the disconnection of g7 by its under-voltage protection. As a result, a sharp decline of the voltage magnitudes is experienced. While a collapse is avoided, the voltage magnitudes settle at unacceptably low values and the case is marked as non-viable. Consequently, the search algorithm does not further expand this $N-2$ contingency sequence.

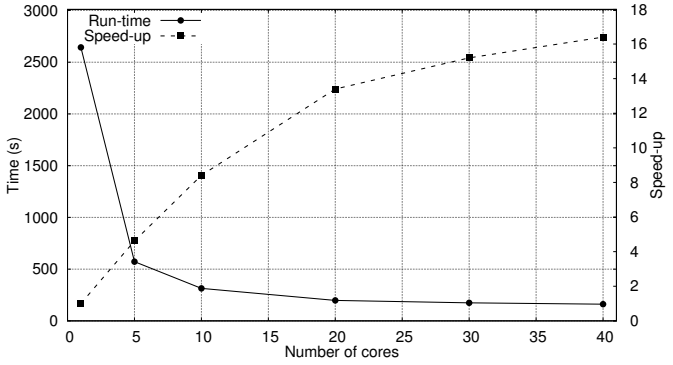

Figure 12. Run-time and speed-up of the algorithm as functions of number of cores. Speed-up is determined with respect to single-core execution.

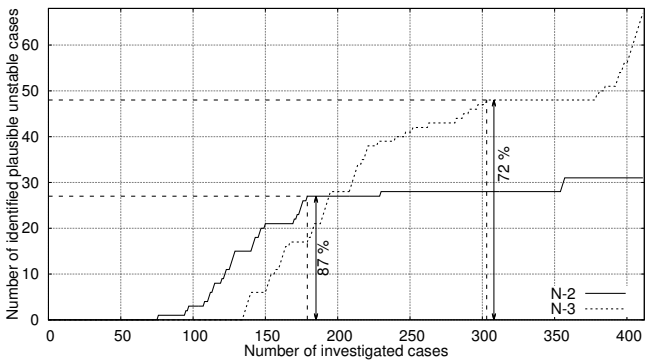

Figure 13. Number of identified unstable $N-2$ and $N-3$ cases as function of number of performed simulations

D. Simulation speed-up

As described in Section II-D, the proposed approach can be implemented into a parallel computing environment. The potential gain in speed-up achieved through parallelization was investigated through repeated executions of the search algorithm and variation of the number of utilized cores between 1 and 40. The simulations were performed on a 48-core AMD Opteron Interlagos (CPU 6238 2.60 GHz, 128 GB RAM) desktop computer running Debian Linux 6.

The initial operating point was in all cases OP B. Figure 12 shows the obtained run-times and speed-up ratios. It can be observed that the run-time decreases from 2643 to 161 s, when increasing the number of cores from one to 40. Moreover, the graph shows that initially an almost linear speed-up can be reached, e.g. with five cores the achieved speed-up is equal to 4.6. When further increasing the number of cores and, hence, workers, a maximum speed-up of around 16 was reached, when using 40 cores.

E. Performance with limited computational resources

In case that the available computational resources are insufficient to investigate all plausible contingencies, the severity index s_i and the sorting of the contingency sequences in L, as described in Section II-E, help first identifying the most severe contingency sequences. In order to assess this feature the number of identified unstable $N-2$ (solid curve) and $N-3$ (dotted curve) contingency sequences as a function of the number of performed simulations are shown in Fig. 13. Operating point B was considered.

For the $N-2$ cases, it can be observed that within the first 180 simulations (44 % of the total number of simulations) 87 % of the plausible unstable cases are identified by the search algorithm. For the $N-3$ cases, it can be observed that only after around 130 performed simulations, the first unstable cases are found. This may be due to the proposed severity index, which leads to first investigating potentially more severe $N-2$ contingency sequences. However, when the first unstable $N-3$ contingency sequences are identified, their number increases progressively and 72 % of the plausible unstable $N-3$ cases are found, after an additional 180 simulations.

IV. Conclusion

In this paper, a practical search algorithm has been proposed for identifying plausible harmful $N-k$ contingency sequences. It employs detailed dynamic time-domain simulations to assess $N-k$ contingency sequences, including cascading events, and identify candidate $(k+1)$-th contingencies. Thus, progressively more severe contingency sequences are assessed. In case of limited computational resources, a severity index allows to prioritize investigation of presumably severe contingency sequences. For speed up of the procedure an implementation into a parallel computing environment was presented.

The proposed method was tested on the IEEE Nordic Test System and the results demonstrated an effective identification of plausible harmful contingencies causing instability or a non-viable system condition. It was demonstrated that the proposed severity index enables earlier identification of harmful contingency sequences and together with parallelization a speed-up of up to 16 could be achieved.

In the future, it is envisioned to test the proposed approach on larger systems. It will be extended to other hidden failures, e.g. malfunctioning of generator under-voltage protection, while alternative severity indices will be investigated.

References

[1] J. Bialek, E. Ciapessoni, D. Cirio, E. Cotilla-Sanchez, C. Dent, I. Dobson, P. Henneaux, P. Hines, J. Jardim, S. Miller, M. Panteli, M. Papic, A. Pitto, J. Quiros-Tortos, and D. Wu, "Benchmarking and validation of cascading failure analysis tools," *IEEE Transactions on Power Systems*, vol. 31, no. 6, pp. 4887–4900, Nov 2016.

[2] D. S. Kirschen and D. P. Nedic, "Consideration of hidden failures in security analysis," in *Proc. 14th PSCC conference, Sevilla*, 2002, pp. 24–28.

[3] D. P. Nedic, "Simulation of large system disturbances," Ph.D. dissertation, University of Manchester, 2003.

[4] B. Otomega, "Distributed and Centralized System Protection Schemes Against Voltage and Thermal Emergencies," Ph.D. dissertation, University of Liège, 2007.

[5] A. Wang, Y. Luo, G. Tu, and P. Liu, "Vulnerability assessment scheme for power system transmission networks based on the fault chain theory," *IEEE Transactions on Power Systems*, vol. 26, no. 1, pp. 442–450, 2011.

[6] M. J. Eppstein and P. D. H. Hines, "A "random chemistry" algorithm for identifying collections of multiple contingencies that initiate cascading failure," *IEEE Transactions on Power Systems*, vol. 27, no. 3, pp. 1698–1705, 2012.

[7] P. Hines, I. Dobson, and P. Rezaei, "Cascading Power Outages Propagate Locally in an Influence Graph that is not the Actual Grid Topology," *IEEE Transactions on Power Systems*, vol. 32, no. 2, pp. 958–967, 2017.
[8] Q. Chen and J. D. McCalley, "Identifying high risk N-k contingencies for online security assessment," *IEEE Transactions on Power Systems*, vol. 20, no. 2, pp. 823–834, 2005.
[9] J. Hazra and A. K. Sinha, "Identification of catastrophic failures in power system using pattern recognition and fuzzy estimation," *IEEE Transactions on Power Systems*, vol. 24, no. 1, pp. 378–387, 2009.
[10] P. F. Petersen, H. Johannsson, and A. H. Nielsen, "Investigation of suitability of cascading outage assessment methods for real-time assessment," in *Proc. 2015 IEEE PowerTech conference, Eindhoven, The Netherlands*, 2015, pp. 13–17.
[11] T. Weckesser and T. Van Cutsem, "Searching for plausible n-k contingencies endangering voltage stability," in *2017 IEEE PES Innovative Smart Grid Technologies Conference Europe (ISGT-Europe)*, Sept 2017, pp. 1–6.
[12] IEEE PES CAMS Task Force, "Initial review of methods for cascading failure analysis in electric power transmission systems," *Proc. IEEE PES General Meeting, 2008*, pp. 1–8, July 2008.
[13] M. Vaiman, K. Bell, Y. Chen, B. Chowdhury, I. Dobson, P. Hines, M. Papic, S. Miller, and P. Zhang, "Risk assessment of cascading outages: Methodologies and challenges," *IEEE Transactions on Power Systems*, vol. 27, no. 2, pp. 631–641, May 2012.
[14] T. Van Cutsem (Chair), "Test Systems for Voltage Stability Analysis and Security Assessment," IEEE PES Power System Dynamic Performance Committee, Tech. Rep. PES-TR19, 2015.